JACS
JOURNAL OF THE AMERICAN CHEMICAL SOCIETY
Communication
pubs.acs.org/JACS

Solvent-Free Synthesis of Zeolites from Anhydrous Starting Raw Solids

Qinming Wu,[†] Xiaolong Liu,[‡] Longfeng Zhu,[§] Lihong Ding,[‡] Pan Gao,[‡] Xiong Wang,[†] Shuxiang Pan,[†] Chaoqun Bian,[†] Xiangju Meng,*[,†] Jun Xu,[‡] Feng Deng,*[,‡] Stefan Maurer,[∥] Ulrich Müller,[∥] and Feng-Shou Xiao*[,†]

[†]Key Lab of Applied Chemistry of Zhejiang Province, Department of Chemistry, Zhejiang University, Hangzhou 310007, P. R. China
[‡]State Key Laboratory of Magnetic Resonance and Atomic and Molecular Physics, Wuhan Center for Magnetic Resonance, Wuhan Institute of Physics and Mathematics, Chinese Academy of Sciences, Wuhan 430071, P. R. China
[§]College of Biological, Chemical Sciences and Engineering, Jiaxing University, Jiaxing 314001, P. R. China
[∥]Process Research and Chemical Engineering, BASF SE, 67056 Ludwigshafen, Germany

Supporting Information

ABSTRACT: Development of sustainable routes for synthesis of zeolites is very important because of wide applications of zeolites at large scale in the fields of catalysis, adsorption, and separation. Here we report a novel and generalized route for synthesis of zeolites in the presence of NH_4F from grinding the anhydrous starting solid materials and heating at 140−240 °C. Accordingly, zeolites of MFI, BEA*, EUO, and TON structures have been successfully synthesized. The presence of F^- drives the crystallization of these zeolites from amorphous phase. Compared with conventional hydrothermal synthesis, the synthesis in this work not only simplifies the synthesis process but also significantly enhances the zeolite yields. These features should be potentially of great importance for industrial production of zeolites at large scale in the future.

Zeolites, a family of microporous silica-based and aluminophosphate-based crystals, have been widely used as catalysts and adsorbents in industrial processes of oil refining and production of fine chemicals due to their high surface area, large pore volume, uniform micropores, and good thermal and hydrothermal stabilities.[1] Usually, zeolite synthesis is performed under hydrothermal, solvothermal, and ionothermal conditions, where a large amount of solvents such as water are necessary.[2−5] The use of the water solvent leads to losses of the nutrients of silicates, aluminosilicates, and aluminophosphates dissolved in the wastewater. As a result, the zeolite yields per given reactor volume are significantly reduced. To overcome this issue, dry gel conversion[4c] and dry synthesis[4d,e] have been successfully developed by Xu's group and Schüth's group. Both routes significantly increase zeolite product yield, but the preparation of starting precursor in the synthesis still requires a large amount of water solvent. The removal of the water solvent in the synthesis still produces polluted wastes. More recently, it has been reported a solvent-free route for synthesis of zeolites, in which the water as solvent could be completely avoided. This route not only effectively increases the zeolite yields but also greatly reduces the production of polluted wastes. However, it is worth noting that this solvent-free synthesis has to use the hydrated form of the solid silica sources.[6] This feature strongly limits industrial applications of conventional anhydrous silica sources in the synthesis of zeolites.[6d] Currently, it still has a challenge for solvent-free synthesis of zeolites from anhydrous starting raw solids.

Initially, hydrothermal synthesis of zeolites was carried out in alkaline media.[2] With the employment of fluoride as mineralizing agent, the hydrothermal synthesis of zeolites was extended to nearly neutral aqueous conditions.[3] In addition, the use of fluoride turned out to be also helpful for the synthesis of silica-rich zeolites.[3]

Here we report a solvent-free synthesis of zeolites from anhydrous starting raw solids in the presence of NH_4F. When tetrapropylammonium bromide (TPABr), tetraethylammonium bromide (TEABr), hexamethonium bromide ($HMBr_2$), and 1-ethyl-3-methylimidazolium bromide ($C_6H_{11}BrN_2$) were employed, pure silica zeolites with MFI, BEA*, EUO, and TON structures can be obtained, respectively. Compared with hydrothermal synthesis, this synthesis route has obvious advantages from a sustainability point of view with respect to simple procedures, high zeolite yields, conventional silica sources, and low-cost organic templates with bromide form.

In a typical run, the solvent-free synthesis of silicalite-1 (S-silicalite-1) from anhydrous starting raw solids in the presence of NH_4F was performed by mechanically grinding of solid silica gel, TPABr, and NH_4F, followed by heating in an autoclave at 180 °C for 15 h. Figure 1a shows the X-ray diffraction (XRD) pattern of the as-synthesized S-silicalite-1, exhibiting the typical peaks associated with MFI-type structure. Figure 1b shows the scanning electron microscopy (SEM) image of the as-synthesized S-silicalite-1, exhibiting almost perfect crystals with uniform morphology. Thermal analysis (TG-DTA) of the as-synthesized S-silicalite-1 displays major exothermic peaks at 250−500 °C accompanied by a weight loss at about 12.37%, which is related to the decomposition of TPABr molecules in the framework (Figure S1). After calcination at 550 °C for 5 h, the calcined S-silicalite-1 shows a typical Langmuir adsorption curve

Received: December 5, 2014
Published: January 9, 2015

DOI: 10.1021/ja5124013
J. Am. Chem. Soc. 2015, 137, 1052−1055

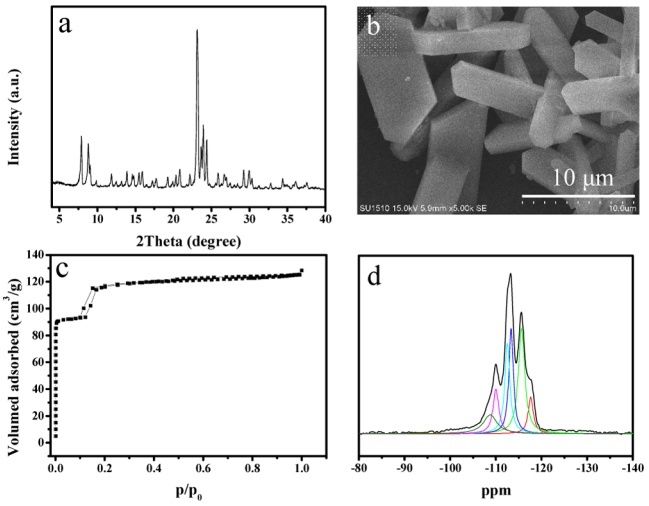

Figure 1. (a) XRD pattern, (b) SEM image, (c) N_2 sorption isotherms, and (d) ^{29}Si NMR spectrum of S-silicalite-1 zeolite. The measurement of the N_2 sorption isotherms is obtained from the calcined S-silicalite-1, and the other measurements are obtained from the as-synthesized S-silicalite-1.

(Figure 1c), which is due to the filling of nitrogen in the micropores of the MFI zeolite. Accordingly, the micropore surface area and micropore volume are estimated to be 423 m^2/g and 0.18 cm^3/g, respectively, which are the same as those of the corresponding zeolite synthesized under hydrothermal conditions. Figure 1d displays the ^{29}Si MAS NMR spectrum of the as-synthesized S-silicalite-1 consisting of signals at −117.6, −115.6, −113.3, −112.5, −110.0, and −108.8 ppm. The former five peaks are assigned to Q^4 silica species [$Si(SiO)_4$], while the peak at −108.8 ppm is attributed to Q^3 silica species [$Si(SiO)_3(OH)$]. The much lower content of Q^3 silica species in the sample suggests that the sample exhibits high crystallinity. The ^{19}F MAS NMR spectrum (Figure S2) displays a major signal at −62.7 ppm, indicating that the fluoride species are almost totally located in the [$4^15^26^2$] cage of the S-silicalite-1 framework.[7]

In the synthesis of S-silicalite-1, it is found that the ratios of NH_4F/SiO_2 and $TPABr/SiO_2$ strongly influence the zeolite crystallization. When the NH_4F/SiO_2 is lower than 0.05 or $TPABr/SiO_2$ is lower than 0.02, the obtained product contains amorphous phase (Figure S3). The suitable NH_4F/SiO_2 and $TPABr/SiO_2$ ratios for the synthesis of S-silicalite-1 are 0.15 and 0.035 (Table S1).

Figure S4 shows XRD patterns and ^{29}Si MAS NMR spectra before and after grinding the mixture of solid silica gel, TPABr, and NH_4F. Interestingly, simple grinding at room temperature results in a weak peak at 18.2° in the XRD pattern, which is assigned to $(NH_4)_2SiF_6$ (Figure S4Ad). Obviously, this compound resulted from an interaction of the solid silica gel with NH_4F. At the same time, an obvious change is observed in the ^{29}Si NMR spectra of the sample before and after grinding at room temperature. After grinding, a large amount of Q^4 silica species is converted into Q^3 silica species in the sample. These results indicate that grinding the anhydrous starting solids leads to a chemical reaction rather than a simple physical mixture, which differs from the report found in the solvent-free synthesis from a hydrated silica source[6a] and the dry synthesis in the presence of NH_4F.[4e] In addition, the XRD peaks associated with TPABr completely disappear, suggesting a high dispersion of TPABr molecules in the mixture,[8] which is in good agreement with the literature.[6a]

Figure 2 displays XRD patterns and ^{29}Si and ^{19}F NMR spectra during the crystallization of S-silicalite-1. The photographs of the samples crystallized at various time in a closed glass tube (Figure S5) show that the samples would always be present as solid phase during the crystallization process, indicating the solid conversion. XRD patterns (Figure 2A) show that weak peaks associated with the MFI structure appear in the sample after heating at 180 °C for 2.5 h, indicating the formation of a small amount of S-silicalite-1, confirmed by the SEM image (Figure S6c). By increasing the crystallization time from 3 to 15 h, the intensity of the XRD peaks gradually increases (Figure 2Ad–h). When the crystallization time exceeds 15 h, no further change in the peak intensity was visible anymore. These results indicate full crystallization at 15 h, confirmed also by SEM (Figure S6h). Figure S7 shows the

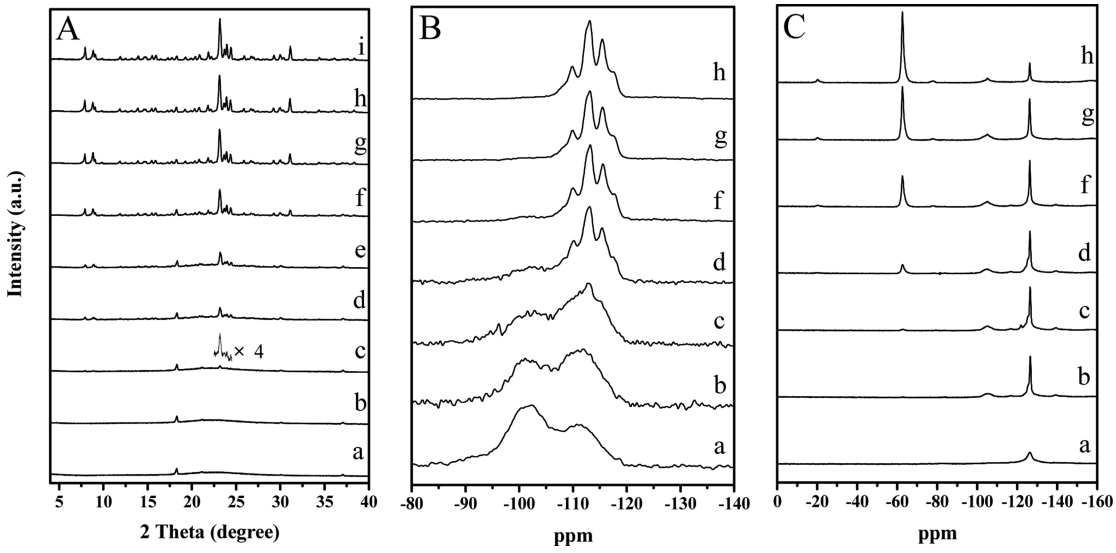

Figure 2. (A) XRD patterns and (B) ^{29}Si and (C) ^{19}F MAS NMR spectra of S-silicalite-1 zeolites crystallized for (a) 0, (b) 2, (c) 2.5, (d) 3, (e) 4.5, (f) 6, (g) 9, (h) 15, and (i) 18 h, respectively.

DOI: 10.1021/ja5124013
J. Am. Chem. Soc. 2015, 137, 1052−1055

dependence of S-silicalite-1 crystallinity over the crystallization time.

Furthermore, ^{29}Si NMR spectra demonstrate the gradual transformation of the Q^3 silica species into Q^4 silica species during the crystallization. ^{19}F NMR spectra show that the anhydrous starting solid mixture exhibits a signal at −126.6 ppm, which is related to the presence of SiF_6^{2-} ions. However, after crystallization time over 2.5 h, an additional new peak at −62.7 ppm appears, which is assigned to the presence of F^- ions in a $[4^15^26^2]$ cage of the MFI structure.[7] Interestingly, this peak intensity gradually increases with the crystallinity, demonstrating the importance of this species for the synthesis of S-silicalite-1. Probably, the transformation of SiF_6^{2-} ions to F^- ions in the $[4^15^26^2]$ cages drives the crystallization of S-silicalite-1 zeolite. The detailed role of the F^- ions during crystallization is currently under investigation.

Figure S8 displays the ^{13}C MAS NMR spectra of the crystallized samples treated with deionized water. This treatment removes the TPABr molecules without interacting with silica species. After crystallization for 2.5 h, the sample exhibits noticeable peaks at 11.4, 16.2, and 63.3 ppm, which are assigned to the presence of TPA^+ ions in the MFI channel. These results indicate that the TPA^+ ions direct the formation of MFI zeolite structure.

After synthesis of S-silicalite-1, this solvent-free synthesis route has been extended to incorporate heteroatoms such as B and Fe into the MFI framework. Figure S9 displays the XRD patterns of heteroatom (such as B and Fe)-substituted ZSM-5 zeolites, showing that these samples have good crystallinity. The coordination of B and Fe atoms in S-B-ZSM-5 and S-Fe-ZSM-5 are studied by solid-state NMR MAS technique and UV−vis spectroscopy, respectively. Figure S10 shows the ^{11}B MAS NMR spectrum of S-B-ZSM-5 zeolite, exhibiting a narrow and symmetric peak at −3.9 ppm, which is typically assigned to $B(SiO)_4$ units in the framework of zeolites.[9] This result unambiguously suggests that the boron atoms have been incorporated into the zeolite framework of S-B-ZSM-5.[9] ICP analysis shows that the Si/B ratio of S-B-ZSM-5 is about 50. Figure S11 shows the UV−vis spectrum of S-Fe-ZSM-5. The sample exhibits a strong band at 241 nm, which is assigned to Fe^{3+} at isolated tetrahedral framework sites (charge transfer bands).[10] Furthermore, three weak absorption bands at 372, 408, and 435 nm could be observed in the magnification spectrum, which are attributed to the weak spin forbidden d−d transitions of Fe^{3+} ion in tetrahedral symmetry.[10] Therefore, the observation of these bands is usually considered as a strong indication for a tetrahedral environment of Fe^{3+} species in the framework of zeolites.[10] ICP analysis shows that the Si/Fe ratio of S-Fe-ZSM-5 is about 31. These results suggest that this synthesis route is also effective for incorporating heteroatoms such as B and Fe into the zeolite framework, which should be important for catalytic applications.

This solvent-free synthesis route has also been employed to prepare other zeolites with BEA*, EUO, and TON structures. The studied syntheses yielded perfect crystals with high crystallinity (Figure 3). After calcination, the organic templates can be removed, allowing access to the microporous structure. After calcination at 550 °C for 5 h, for example, pure silica S-beta exhibits a typical Langmuir-type sorption curve (Figure S12) with a surface area of 511 m^2/g and a pore volume of 0.23 cm^3/g. These values are comparable with those of pure silica-beta synthesized via conventional hydrothermal route. Currently, this

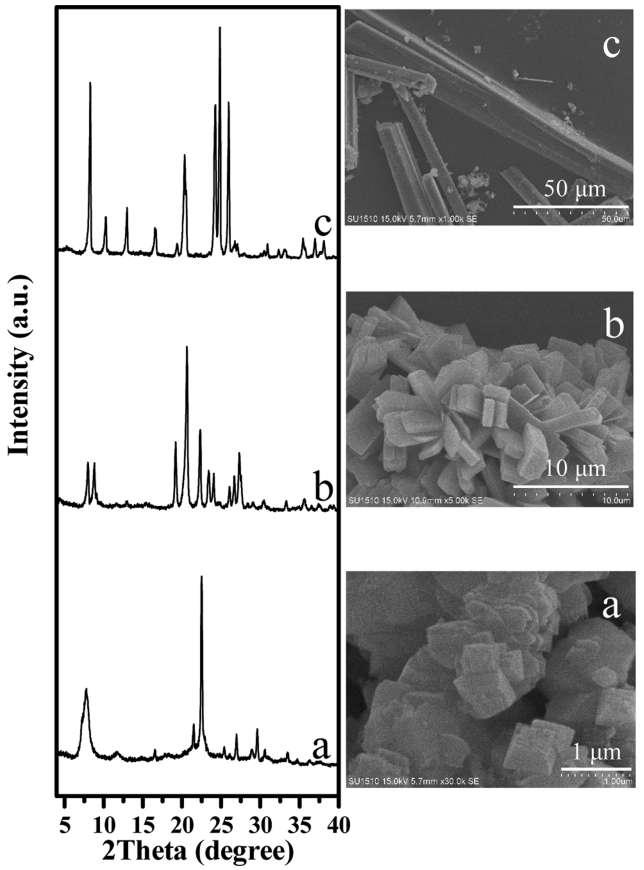

Figure 3. XRD patterns (left) and SEM images (right) of (a) BEA*, (b) EUO, and (c) TON zeolites.

solvent-free synthesis route is applied to synthesize various other zeolite structures employing different organic templates.

Compared to conventional hydrothermal synthesis, the synthesis route here has obvious advantages as follows: (1) very simple procedures for the synthesis, consisting of only grinding and heating; (2) very high zeolite yield due to full utilization of the autoclave volume, for example, when 3.20 g of SiO_2 sources was crystallized in 15 mL of an autoclave, 3.06 g of S-silicate-1 product was obtained; (3) the use of conventional anhydrous silica sources such as solid silica gel; (4) the use of low-cost organic templates. Pure silica zeolites in general were typically synthesized using the hydroxide form of the organic templates. However, in this work all pure silica zeolites could be synthesized in the presence of the bromide form of the organic templates. The bromide form has much lower cost than the hydroxide form of the organic templates owing to their easier production, making this route also highly attractive from an economic perspective. For example, pure silica BEA* structure has not been successfully synthesized in the bromide form of the organic templates except for this work. These features are favorable for sustainable synthesis of zeolites.

In summary, zeolites with MFI, BEA*, EUO, and TON structures have been successfully synthesized via solvent-free synthesis including a grinding step at room temperature, followed by crystallization at 140−240 °C of the anhydrous solid mixture consisting of solid silica gel, NH_4F, and organic templates. As a typical example, the synthesis of S-silicalite-1 zeolite with MFI structure was investigated in detail. The ^{19}F NMR spectroscopy demonstrates that the transformation of SiF_6^{2-} ions to F^- ions located in the $[4^15^26^2]$ cages of the

DOI: 10.1021/ja5124013
J. Am. Chem. Soc. 2015, 137, 1052−1055

framework plays an important role for the crystallization of S-silicalite-1.

■ ASSOCIATED CONTENT

Supporting Information

Synthesis and characterization details. This material is available free of charge via the Internet at http://pubs.acs.org.

■ AUTHOR INFORMATION

Corresponding Authors

*mengxj@zju.edu.cn
*dengf@wipm.ac.ccn
*fsxiao@zju.edu.cn

Notes

The authors declare no competing financial interest.

■ ACKNOWLEDGMENTS

This work is supported by the NSFC China (21422306, 21333009, 21273197, and 21210005).

■ REFERENCES

(1) (a) Davis, M. E.; Lobo, R. F. *Chem. Mater.* **1992**, *4*, 756. (b) Gies, H.; Marler, B. *Zeolite* **1992**, *12*, 42. (c) Davis, M. E. *Nature* **2002**, *417*, 813. (d) Cundy, C. S.; Cox, P. A. *Chem. Rev.* **2003**, *103*, 663. (e) Moller, K.; Bein, T. *Chem. Soc. Rev.* **2013**, *42*, 3689. (f) Moliner, M.; Rey, F.; Corma, A. *Angew. Chem., Int. Ed.* **2013**, *52*, 13880. (g) Mintova, S.; Gilson, J. P.; Valtchev, V. *Nanoscale* **2013**, *5*, 6693. (h) Davis, M. E. *Chem. Mater.* **2014**, *26*, 239. (i) Moliner, M.; Martínez, C.; Corma, A. *Chem. Mater.* **2014**, *26*, 246. (j) Meng, X. J.; Xiao, F.-S. *Chem. Rev.* **2014**, *114*, 1521.

(2) (a) Breck, D. W. *Zeolite Molecular Sieves*; Wiley: New York, 1974. (b) Barrer, R. M. *Zeolites and Clay Minerals as Sorbents and Molecular Sieves*; Academic Press: London, 1978. (c) Barrer, R. M. *Hydrothermal Chemistry of Zeolites*; Academic Press: London, 1982.

(3) (a) Guth, J. L.; Kessler, H.; Higel, J. M.; Lamblin, J. M.; Patarin, J.; Seive, A.; Chezeau, J. M.; Wey, R. *ACS Symp. Ser.* **1989**, *398*, 176. (b) Caullet, P.; Hazm, J.; Guth, J. L.; Joly, J. F.; Lynch, J.; Raatz, F. *Zeolites* **1992**, *12*, 240. (c) Dwyer, J.; Zhao, J. P. *J. Mater. Chem.* **1992**, *2*, 235. (d) Camblor, M. A.; Corma, A.; Valencia, S. *Chem. Commun.* **1996**, *20*, 2365. (e) Diaz-Cabanas, M. J.; Camblor, M. A.; Liu, Z.; Ohsuna, T.; Terasaki, O. *J. Mater. Chem.* **2002**, *12*, 249. (f) Cantin, A.; Corma, A.; Diaz-Cabanas, M. J.; Jorda, J. L.; Moliner, M. *Angew. Chem., Int. Ed.* **2006**, *45*, 8013. (g) Rojas, A.; Gomez-Hortiguela, L.; Camblor, M. A. *J. Am. Chem. Soc.* **2012**, *134*, 3845. (h) Rojas, A.; Martinez-Morales, E.; Zicovich-Wilson, C. M.; Camblor, M. A. *J. Am. Chem. Soc.* **2012**, *134*, 2255. (i) Hould, N.; Haouas, M.; Nikolakis, V.; Taulelle, F.; Lobo, R. *Chem. Mater.* **2012**, *24*, 3621.

(4) (a) Xu, R.; Pang, W.; Yu, J.; Huo, Q.; Chen, J. *Chemistry of Zeolite and Related Porous Materials*; Wiley: Singapore, 2007. (b) Bibby, D. M.; Dale, M. P. *Nature* **1985**, *317*, 157. (c) Xu, W. Y.; Dong, J. X.; Li, J. P.; Li, J. Q.; Wu, F. *J. Chem. Soc. Chem. Commun.* **1990**, *10*, 755. (d) Althoff, R.; Unger, K.; Schüth, F. *Microporous Mater.* **1994**, *2*, 557. (e) Deforth, U.; Unger, K. K.; Schüth, F. *Microporous Mater.* **1997**, *9*, 287. (f) Hong, S. B.; Min, H. K.; Shin, C. H.; Cox, P. A.; Warrender, S. J.; Wright, P. A. *J. Am. Chem. Soc.* **2007**, *129*, 10870. (g) Shin, J.; Camblor, M. A.; Woo, H. C.; Miller, S. R.; Wright, P. A.; Hong, S. B. *Angew. Chem., Int. Ed.* **2009**, *48*, 6647. (h) Na, K.; Jo, C.; Kim, J.; Cho, K.; Jung, J.; Seo, Y.; Messinger, R. J.; Chmelka, B. F.; Ryoo, R. *Science* **2011**, *333*, 328. (i) Moliner, M.; Gonzalez, J.; Portilla, M. T.; Willhammar, T.; Rey, F.; Liopis, F. J.; Zou, X. D.; Corma, A. *J. Am. Chem. Soc.* **2011**, *133*, 9497. (j) Itabashi, K.; Kamimura, Y.; Iyoki, K.; Shimojima, A.; Okubo, T. *J. Am. Chem. Soc.* **2012**, *134*, 11542. (k) Zhang, X. Y.; Liu, D. X.; Xu, D. D.; Asahina, S.; Cychosz, K. A.; Agrawal, K. V.; Al Wahedi, Y.; Bhan, A.; Al Hashimi, S.; Terasaki, O.; Thommes, M.; Tsapatsis, M. *Science* **2012**, *336*, 1684. (l) Park, M. B.; Lee, Y.; Zheng, A. M.; Xiao, F. S.; Nicholas, C. P.; Lewis, G. J.; Hong, S. B. *J. Am. Chem. Soc.* **2013**, *135*, 2248. (m) Xie, D.; McCusker, L. B.; Baerlocher, C.; Zones, S. I.; Wan, W.; Zou, X. D. *J. Am. Chem. Soc.* **2013**, *135*, 10519. (n) Wu, Q. M.; Wang, X.; Meng, X. J.; Yang, C. G.; Liu, Y.; Jin, Y. Y.; Yang, Q.; Xiao, F.-S. *Microporous Mesoporous Mater.* **2014**, *186*, 106. (o) Wang, Q.; Cui, Z. M.; Cao, C. Y.; Song, W. G. *J. Phys. Chem. C* **2011**, *115*, 24987. (p) Qin, Z.; Shen, B.; Yu, Z.; Deng, F.; Zhao, L.; Zhou, S.; Yuan, D.; Gao, X.; Wang, B.; Zhao, H.; Liu, H. *J. Catal.* **2013**, *298*, 102.

(5) (a) Cooper, E. R.; Andrews, C. D.; Wheatley, P. S.; Webb, P. B.; Wormald, P.; Morris, R. E. *Nature* **2004**, *430*, 1012. (b) Xu, Y.; Tian, Z.; Wang, S.; Hu, Y.; Wang, L.; Wang, B.; Ma, Y.; Hou, L.; Yu, J.; Lin, L. *Angew. Chem., Int. Ed.* **2006**, *45*, 3965. (c) Parnham, E. R.; Morris, R. E. *J. Am. Chem. Soc.* **2006**, *128*, 2204. (d) Cai, R.; Liu, Y.; Gu, S.; Yan, Y. *J. Am. Chem. Soc.* **2010**, *132*, 12776. (e) Wheatley, P. S.; Allan, P. K.; Teat, S. J.; Ashbrook, S. E.; Morris, R. E. *Chem. Sci.* **2010**, *1*, 483.

(6) (a) Ren, L. M.; Wu, Q. M.; Yang, C. G.; Zhu, L. F.; Li, C. J.; Zhang, P. L.; Zhang, H. Y.; Meng, X. J.; Xiao, F.-S. *J. Am. Chem. Soc.* **2012**, *134*, 15173. (b) Morris, R. E.; James, S. L. *Angew. Chem., Int. Ed.* **2013**, *52*, 2163. (c) Wu, Q. M.; Wang, X.; Qi, G. D.; Guo, Q.; Pan, S. X.; Meng, X. J.; Xu, J.; Deng, F.; Fan, F. T.; Feng, Z. C.; Li, C.; Maurer, S.; Müller, U.; Xiao, F.-S. *J. Am. Chem. Soc.* **2014**, *136*, 4019. (d) Mahmoud, E.; Lobo, R. F. *Microporous Mesoporous Mater.* **2014**, *189*, 97.

(7) (a) Fyfe, C. A.; Brouwer, D. H.; Lewis, A. R.; Chézeau, J. M. *J. Am. Chem. Soc.* **2001**, *123*, 6882. (b) Villaescusa, L. A.; Bull, I.; Wheatley, P. S.; Lightfoot, P.; Morris, R. E. *J. Mater. Chem.* **2003**, *13*, 1978. (c) Liu, X. L.; Ravon, U.; Tuel, A. *Angew. Chem., Int. Ed.* **2011**, *50*, 5900.

(8) Xiao, F.-S.; Zheng, S.; Sun, J. M.; Yu, R. B.; Qiu, S. L.; Xu, R. R. *J. Catal.* **1998**, *176*, 474.

(9) (a) Zhu, Q.; Hinode, M.; Yokoi, T.; Yoshika, M.; Kondo, J. N.; Tatsumi, T. *Catal. Commun.* **2009**, *10*, 447. (b) Chen, L.; Zhang, M.; Yue, Y.; Ye, C.; Deng, F. *Microporous Mesoporous Mater.* **2004**, *76*, 151. (c) Yokoi, T.; Yoshioka, M.; Imai, H.; Tatsumi, T. *Angew. Chem., Int. Ed.* **2009**, *48*, 9884.

(10) (a) Bordiga, S.; Buzzoni, R.; Geobaldo, F.; Lamberti, C.; Giamello, E.; Zecchina, A.; Leofanti, G.; Petrini, G.; Tozzola, G.; Vlaic, G. *J. Catal.* **1996**, *158*, 486. (b) Hensen, E. J. M.; Zhu, Q.; Janssen, R. A. J.; Magusin, P. C. M. M.; Kooyman, P. J.; van Santen, R. A. *J. Catal.* **2005**, *233*, 123. (c) Guo, D.; Shen, B.; Qi, G.; Zhao, L.; Xu, J.; Deng, F.; Qin, Y.; Guo, Q.; Ren, S.; Gao, X.; Qin, S.; Wang, B.; Zhao, H.; Liu, H.; Pang, X. *Chem. Commun.* **2014**, *50*, 2660.

DOI: 10.1021/ja5124013
J. Am. Chem. Soc. 2015, 137, 1052−1055